

Chapter 4

Pure Phase NMR

In traditional liquid state NMR pure-phase spectra have always been important in giving the highest signal-to-noise ratios and signal resolution. The basic problem is most easily illustrated with a simple two-dimensional data set of the form $S(t_1, t_2)$ (notice the similarity between this equation and equation 3.7).

$$S(t_1, t_2) = e^{-T_2^{-1}(t_1+t_2)} e^{-i\Omega_1 t_1} e^{-i\Omega_2 t_2} \quad (4.1)$$

Where Ω_1 and Ω_2 are the frequencies in each dimension for a single peak in the 2D Fourier transformed spectrum with linewidth $1/2T_2$. When a 2D data set of this form is Fourier transformed in the t_2 dimension, the result is a data set of the form $S(t_1, \omega_2)$.

$$S(t_1, \omega_2) = e^{-T_2^{-1} t_1} e^{-i\Omega_1 t_1} \left(A(\omega_2, \Omega_2) + iD(\omega_2, \Omega_2) \right) \quad (4.2)$$

Where $A(\omega, \Omega)$ and $D(\omega, \Omega)$ in this case are the absorptive and dispersive Lorentzian lineshape functions respectively with a peak in the ω dimension at frequency Ω .

$$\begin{aligned} A(\omega, \Omega) &= \frac{T_2}{1+(\omega-\Omega)^2 T_2^2} \\ D(\omega, \Omega) &= \frac{(\omega-\Omega)T_2^2}{1+(\omega-\Omega)^2 T_2^2} \end{aligned} \quad (4.3)$$

It is immediately apparent, that the second Fourier transform will produce a very complex result, $S(\omega_1, \omega_2)$.

$$\begin{aligned} S(\omega_1, \omega_2) &= \left(A(\omega_1, \Omega_1) + iD(\omega_1, \Omega_1) \right) \left(A(\omega_2, \Omega_2) + iD(\omega_2, \Omega_2) \right) \\ &= \left(A(\omega_1, \Omega_1)A(\omega_2, \Omega_2) - D(\omega_1, \Omega_1)D(\omega_2, \Omega_2) \right) \\ &\quad + i \left(A(\omega_1, \Omega_1)D(\omega_2, \Omega_2) + D(\omega_1, \Omega_1)A(\omega_2, \Omega_2) \right) \end{aligned} \quad (4.4)$$

This has two terms, one real and one imaginary. If this were completely pure-absorptive mode, the real term would contain $A(\omega_1, \Omega_1)A(\omega_2, \Omega_2)$ only. The term which leads to the phase-twist lineshape is the $A(\omega_1, \Omega_1)A(\omega_2, \Omega_2) - D(\omega_1, \Omega_1)D(\omega_2, \Omega_2)$ one. Figure 4.1 shows both the pure-absorption mode and phase-twist 2D lineshapes. The next sec-

tion describes three of the methods used to obtain a pure-absorptive mode lineshape in

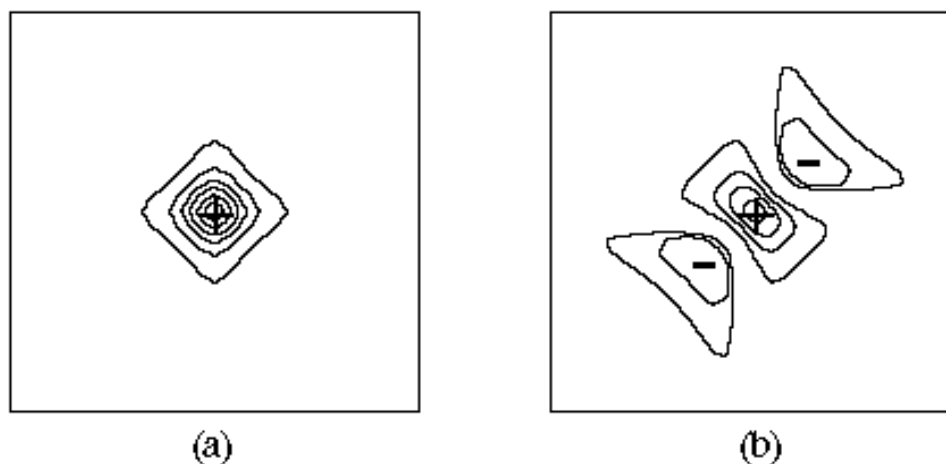


Figure 4.1 Pure-Absorption mode and Mixed-Phase 2D NMR Spectra. Spectrum (a) is an example of a pure-absorption mode line with equal homogeneous broadening in both dimensions. Spectrum (b) is an example of a mixed-phase line with the same parameters. Note in (b) the presence of both positive (+) and (-) contours, giving a peak of much larger effective linewidth.

2D NMR experiments. Each will be described briefly and in all cases additional information may be found in the papers referenced therein and in the classic text on multi-dimensional NMR by Ernst *et al.*⁷

Pure-Absorption Mode Acquisition Methods

The three most important methods for achieving pure-absorption phase multi-dimensional NMR data, States, TPPI and whole echo acquisition, are described in moderate detail in the next section. Each section contains references to other more complete descriptions of these experiments and the interested reader is directed there for additional information.

States Method

The method developed by States *et al.*⁸⁸ creates pure-absorption mode spectra by acquiring a hypercomplex data set. In this type of data acquisition, there are two parts, a

cosine labeled $S_c(t_1, t_2)$ and a sine labeled $S_s(t_1, t_2)$ portion. Thus, twice as many data points are needed to get the same resolution as a comparable phase-modulated experiment. The hypercomplex data is collected such that the cosine portion is quadrature in t_2 and amplitude modulated by $\cos(\Omega_1 t_1)$ in t_1 while the sine portion is amplitude modulated by $\sin(\Omega_1 t_1)$ in t_1 . Mathematically, the two signals are expressed in equation 4.5.

$$\begin{aligned} S_c(t_1, t_2) &= \cos(\Omega_1 t_1) e^{-T_2^{-1}(t_1 + t_2)} e^{-i\Omega_2 t_2} \\ S_s(t_1, t_2) &= \sin(\Omega_1 t_1) e^{-T_2^{-1}(t_1 + t_2)} e^{-i\Omega_2 t_2} \end{aligned} \quad (4.5)$$

To process this type of data, the t_2 Fourier transform is performed separately on each data set. This yields two new signal functions $S_c(t_1, \omega_2)$ and $S_s(t_1, \omega_2)$ given below.

$$\begin{aligned} S_c(t_1, \omega_2) &= \cos(\Omega_1 t_1) e^{-T_2^{-1} t_1} (A(\omega_2, \Omega_2) + iD(\omega_2, \Omega_2)) \\ S_s(t_1, \omega_2) &= \sin(\Omega_1 t_1) e^{-T_2^{-1} t_1} (A(\omega_2, \Omega_2) + iD(\omega_2, \Omega_2)) \end{aligned} \quad (4.6)$$

These are then combined to form a data set $S_{pp}(t_1, \omega_2)$ whose real components are the real portion of $S_c(t_1, \omega_2)$ and whose imaginary components are the negated real portion of $S_s(t_1, \omega_2)$.

$$\begin{aligned} S_{pp}(t_1, \omega_2) &= A(\omega_2, \Omega_2) e^{-T_2^{-1} t_1} (\cos(\Omega_1 t_1) - i \sin(\Omega_1 t_1)) \\ &= A(\omega_2, \Omega_2) e^{-T_2^{-1} t_1} e^{-i\Omega_1 t_1} \end{aligned} \quad (4.7)$$

This data set is now ready to be Fourier transformed with respect to t_1 . Notice that there is no dispersive $D(\omega_2, \Omega_2)$ term in the $S_{pp}(t_1, \omega_2)$ expression. In fact the final $S_{pp}(\omega_1, \omega_2)$ will have no dispersive contribution to the real channel (which is what normally is displayed).

$$S_{pp}(\omega_1, \omega_2) = A(\omega_1, \Omega_1) A(\omega_2, \Omega_2) + iD(\omega_1, \Omega_1) A(\omega_2, \Omega_2) \quad (4.8)$$

This will yield a truly pure-absorption mode lineshape, such as in figure 4.1. To implement a phase cycle to collect this type of hypercomplex data set, the data must be collected with both the +1 and -1 coherence pathways in t_1 . When summed together they yield a cosine pathway and when subtracted they yield a sine pathway. A simple method

for deriving a phase cycle for a hypercomplex data set is to take a phase cycle which chooses only the -1 or $+1$ pathway in t_1 and split this cycle into two phase cycles. One will be made up of those cycles which generate cosine in t_1 and the other will have those which generate sine in t_1 . This is a little more difficult when t_1 is split between two different evolution periods (such as the original DAS experiment), but can still be accomplished with proper phase cycling and pulses (see Mueller *et al.*⁵⁰)

Time Proportional Phase Incrementation

The technique of time proportional phase incrementation (TPPI)^{89,90} is mathematically equivalent to the method derived by States. Again, twice as many data points must be collected as in a phase-modulated experiment with the same resolution. The basic difference between States method and TPPI arises in the data acquisition and processing. To acquire TPPI data, a $S_{TPPI}(t_1, t_2)$ data set is collected where the dwell time t_1 is one half and the number of t_1 points is twice what would be normally used in a phase modulated experiment, giving both the same spectral width and digital resolution in t_1 . In addition, all the pulses immediately before the t_1 evolution period begins are incremented by 90° after each t_1 point.

$$S_{TPPI}(t_1, t_2) = e^{-T_2^{-1}(t_1+t_2)} \cos\left(\Omega_1 t_1 + \frac{\pi t_1}{2\Delta t_1}\right) e^{i\Omega_2 t_2} \quad (4.9)$$

This data is Fourier transformed with respect to t_2 exactly as a usual phase modulated data set to yield $S_{TPPI}(t_1, \omega_2)$.

$$\begin{aligned} S_{TPPI}(t_1, \omega_2) &= e^{-T_2^{-1}t_1} \cos\left(\left(\Omega_1 + \frac{\pi}{2\Delta t_1}\right)t_1\right) \left(A(\omega_2, \Omega_2) + iD(\omega_2, \Omega_2)\right) \\ &= e^{-T_2^{-1}t_1} A(\omega_2, \Omega_2) \cos\left(\left(\Omega_1 + \frac{\pi}{2\Delta t_1}\right)t_1\right) + \\ &\quad iD(\omega_2, \Omega_2) \cos\left(\left(\Omega_1 + \frac{\pi}{2\Delta t_1}\right)t_1\right) \end{aligned} \quad (4.10)$$

The imaginary portion of this data set is then thrown out and the remaining real portion is Fourier transformed with a real Fourier transform in t_1 (rather than the usual complex

Fourier transform). This type of Fourier transform has no quadrature and peaks show up at both the positive and negative frequencies. This is where the phase incrementation "trick" can be seen. Each term has a ω_1 frequency of $\Omega_1 + \frac{\pi}{2\Delta t_1}$ rather than just Ω_1 . Therefore the signal will be given by equation 4.11.

$$S_{TPPI}(\omega_1, \omega_2) = \begin{aligned} & A(\omega_2, \Omega_2) \left(A\left(\omega_1, \Omega_1 + \frac{\pi}{2\Delta t_1}\right) + A\left(\omega_1, -\Omega_1 - \frac{\pi}{2\Delta t_1}\right) \right) - \\ & iA(\omega_2, \Omega_2) \left(D\left(\omega_1, \Omega_1 + \frac{\pi}{2\Delta t_1}\right) + D\left(\omega_1, -\Omega_1 - \frac{\pi}{2\Delta t_1}\right) \right) \end{aligned} \quad (4.11)$$

The resulting spectrum is symmetric about zero frequency and the negative side may now be thrown out. The remaining positive frequency data set is pure-absorption mode and may be made equivalent to the States result by setting the center of the spectrum to zero frequency (a shift of $\frac{\pi}{2\Delta t_1}$). The phase cycle for this type of spectrum is identical to the phase cycle for the cosine portion of the hypercomplex data set from the previous section with the addition of the time proportional phase incrementation of the pulses before the start of t_1 .

Whole Echo Acquisition

Whole echo acquisition⁹¹ has been less popular than the other methods of obtaining pure phase spectra. This is primarily because in the case of liquid spectra, it is difficult to obtain whole echoes in t_2 since the lines are so narrow. In fact, when only a fraction of the echo is collected phase twist components will enter into the final 2D spectrum. In the case of solids, where the inhomogeneous broadening is usually much larger than the homogeneous broadening, whole echo acquisition can actually be better than the other methods. To understand why two-dimensional whole echo acquisition works, first it is useful to look at a one-dimensional case. Suppose you generate a Gaussian-shaped time-domain echo with a 90° - 180° (t_e - t_e - t_e - t_e) sequence which has a signal $S_e(t_2)$ given by equation 4.12.

$$S_e(t_2) = e^{-T_2^{-2}(t_2-t_e)^2} e^{-i\Omega_2(t_2-t_e)} \quad (4.12)$$

When this signal is Fourier transformed, a spectrum of the form given by equation 4.13 will be generated, assuming that the signal is shifted far enough out in time and is zero at both the first and last t_2 points.

$$S_e(\omega_2) = e^{-\frac{(\omega_2 - \Omega_2)^2 T_2^2}{4}} e^{i\omega t_e} = A_e(\omega_2, \Omega_2) \quad (4.13)$$

This appears at first glance to be much worse than if we had only collected from the echo top on, due to the phase factor. However, by effectively shifting the time origin by applying a first-order phase correction of t_e (which multiplies each point in the spectrum by $e^{-i\omega t_e}$), the spectrum is greatly simplified.

$$S_{se}(\omega_2) = e^{-\frac{(\omega_2 - \Omega_2)^2 T_2^2}{4}} = A_{se}(\omega_2, \Omega_2) \quad (4.14)$$

This shifted-echo (hence the *se* subscript) spectrum has no dispersive imaginary components. This can be quite useful in a two-dimensional experiment where the signal is of the form.

$$S_e(t_1, t_2) = e^{-T_2^{-2}(t_2-t_e)^2} e^{-i\Omega_2(t_2-t_e)} e^{-T_2^{-1}t_1} e^{-i\Omega_1 t_1} \quad (4.15)$$

This is a constant time echo experiment and the first Fourier transform is done as usual in the t_2 dimension. The resulting signal function has the form given in equation 4.16.

$$S_e(t_1, \omega_2) = A_e(\omega_2, \Omega_2) e^{-T_2^{-1}t_1} e^{-i\Omega_1 t_1} \quad (4.16)$$

A first order phase correction of t_e is then applied to the ω_2 dimension which yields signal with the function given in equation 4.17 (note the *se* subscript on the absorptive one-dimensional $A_{se}(\omega_2, \Omega_2)$ function).

$$S_{se}(t_1, \omega_2) = A_{se}(\omega_2, \Omega_2) e^{-T_2^{-1}t_1} e^{-i\Omega_1 t_1} \quad (4.17)$$

A Fourier transform is then applied to the t_1 dimension giving a pure-absorption mode 2D spectrum as the result (see equation 4.18).

$$S_e(\omega_1, \omega_2) = A_{se}(\omega_2, \Omega_2) \left(A(\omega_1, \Omega_1) + iD(\omega_1, \Omega_1) \right) \quad (4.18)$$

This result is particularly important because data of this sort doesn't require the factor of 2 additional t_1 points like the States or TPPI methods, thus it will have a $\sqrt{2}$ improvement in signal-to-noise over States or TPPI data. However, this is only true in situations where the entire echo may be collected for every t_1 point, which in general will only be the case for solids with a strong inhomogeneous broadening. The phase cycle necessary to collect a whole echo is not any different than collecting a standard phase-modulated data set. In fact, in some cases TPPI or States methods may be applied in concert with whole echo acquisition to gain an additional $\sqrt{2}$ improvement in signal-to-noise ratio.⁵³

Pure Phase DAS

The original DAS experiment as described by both Mueller *et al.*⁴² and Llor and Virlet⁴³ was a phase modulated experiment (with the phase cycles given in the papers) and gave phase-twist lineshapes in two dimensional spectra which necessitated magnitude mode display (see figure 3.6). To obtain higher resolution, pure-phase two dimensional DAS experiments were first developed by Mueller *et al.*^{42,47} In this work, they viewed the DAS experiment in a non-sheared fashion and used either a z-filter or a 90° pulse after the total t_1 evolution period to give pure-absorption mode spectra. As will be discussed below, we have been able to obtain higher signal to noise ratio pure-absorption mode DAS spectra by redefining our time axes.⁵³ Also, further sensitivity improvements have been made by shifting the DAS echo in time using π pulses.

Pulse Sequences

The original DAS pulse sequence has been discussed earlier but will be reviewed to show the differences between it and the new pulse sequences. In figure 4.2 we see a simulated DAS spectrum acquired with the original DAS sequence. The mixed-phase artifacts are seen in the upper right and lower left side of the spectrum as broad negative re-

gions. This overall phase twist will make the slices through the isotropic peaks difficult to interpret.

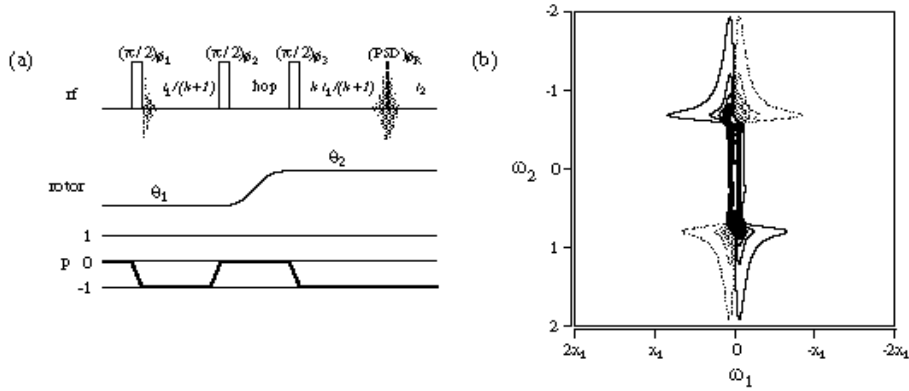


Figure 4.2 Original DAS Experiment. The pulse sequence and coherence pathway (a) is shown to the left of the simulated spectrum (b). The phase cycle used to implement this pathway was given earlier. Dashed contour lines indicate negative contours.

Figure 4.3 shows the modified DAS experiment where the time axes have been redefined, very similar to the time definitions in a 2D exchange experiment (and identical to those definitions discussed in the description of spinning sidebands in chapter 3). In this experiment, the evolution at the first angle is defined as t_1 and the evolution after the hop is defined as t_2 . This definition will place a shifting DAS isotropic echo in the t_2 dimension. In fact, this echo will appear at a time $k t_1$. When this data is processed without modification, we observe a diagonal peak which is the correlation between anisotropic patterns in both dimensions. A conventional 2D DAS spectrum may be obtained by shearing this spectrum by an angle θ_s (as was mentioned earlier in the spinning sidebands section of chapter 3).

$$\theta_s = \tan^{-1} k \quad (4.19)$$

Another method for shearing the data is to apply a t_1 dependent first-order phase correction of $\phi(t_1, \omega_2)$ to the data set between the first and second Fourier transforms.

$$\begin{aligned} \phi(t_1, \omega_2) &= k \omega_2 t_1 \\ S(t_1, \omega_2) &= e^{-i\phi(t_1, \omega_2)} S(t_1, \omega_2) \end{aligned} \quad (4.20)$$

This method of acquisition produces a phase-twist spectrum, but because an entire echo is collected for the later t_1 points, the negative contours are much smaller, giving effectively higher resolution in both dimensions.

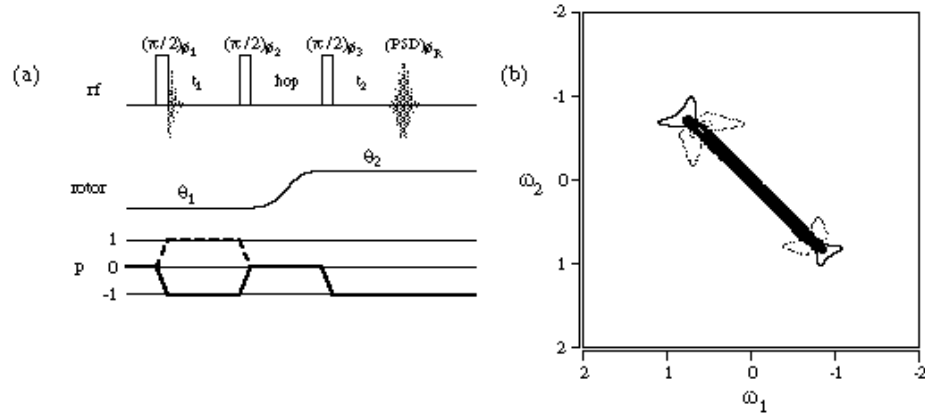


Figure 4.3 Modified DAS Experiment. The (a) pulse sequence and coherence pathway are shown to the left of (b) the unsheared simulated spectrum. The dashed line coherence pathway indicates the anti-echo DAS experiment. The phase cycle used to implement this pathway is identical to the original DAS experiment. Dashed contour lines indicate negative contours.

A second modification to the DAS experiment may be made by using either the method of States *et al.*⁸⁸ or TPPI^{89,90} to acquire pure-absorption mode spectra using the same t_1 and t_2 definitions. To accomplish this, we need to merely change the way the data is collected. Rather than collecting a single data set as a function of t_1 and t_2 , we collect a hypercomplex data set as a function of t_1 and t_2 . As mentioned previously, a hypercomplex data set separates the sine and cosine evolution in t_1 . Each of these data sets is Fourier transformed with respect to t_2 . This produces a data set with absorptive lineshapes in the real channel and dispersive lineshapes in the imaginary channel. The real portion of the cosine data set is combined with $\sqrt{-1}$ times the real portion of the sine data set. Thus there are only absorptive lineshapes in ω_2 which are modulated by $e^{-i\Omega_1 t_1}$ in the t_1 dimension. Applying the same t_1 dependent first-order phase correction from equation 4.2, we then can perform the t_1 Fourier transform. This yields pure-absorption mode 2D DAS spectra. There are no mixed-phase artifacts to make interpretation difficult. The phase cycle and coherence pathway for this experiment are given in figure 4.4.

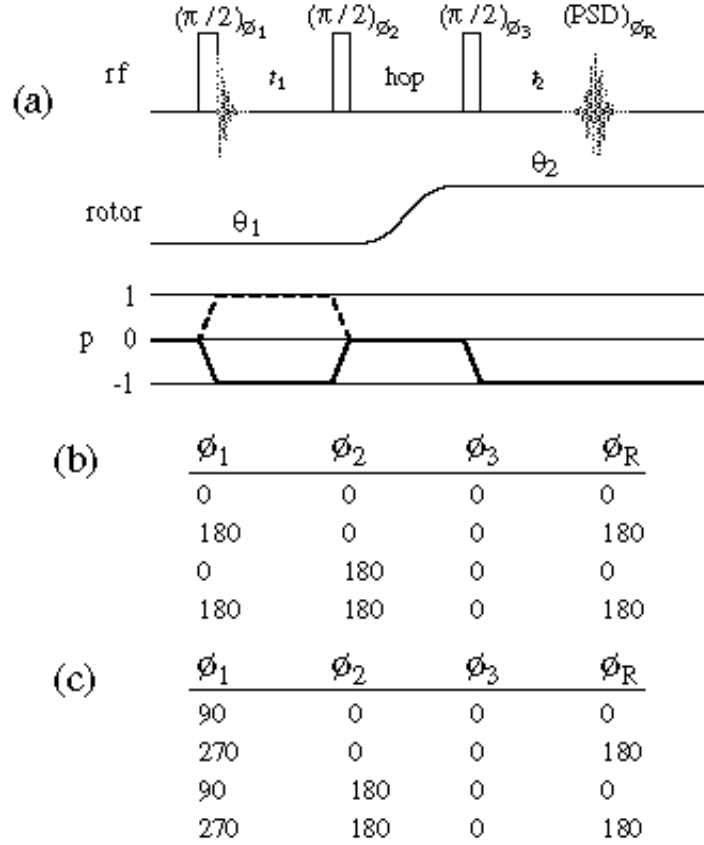


Figure 4.4 Hypercomplex DAS Experiment. The pulse sequence (a), coherence pathway, and phase cycle are given above. Cycle (b) is the cosine data set and cycle (c) is the sine data set.

An alternative method of sensitivity improvement in dynamic-angle spinning experiments comes from shifting the isotropic DAS echo in t_2 . This is accomplished by applying a π pulse after a $n t_r$ delay following the final $\pi/2$ read pulse. This shifted echo DAS (SEDAS) pulse sequence is detailed in figure 4.5. This sequence has the advantage of shifting the DAS echoes in time by $n t_r$. For all t_1 values, an entire DAS echo may be collected which leads to a higher signal-to-noise ratio than the hypercomplex DAS which takes twice as long to effectively collect whole echoes in t_1 . This is especially important in cases where the broadening is primarily inhomogeneous and anisotropic in the ω_2 dimension.

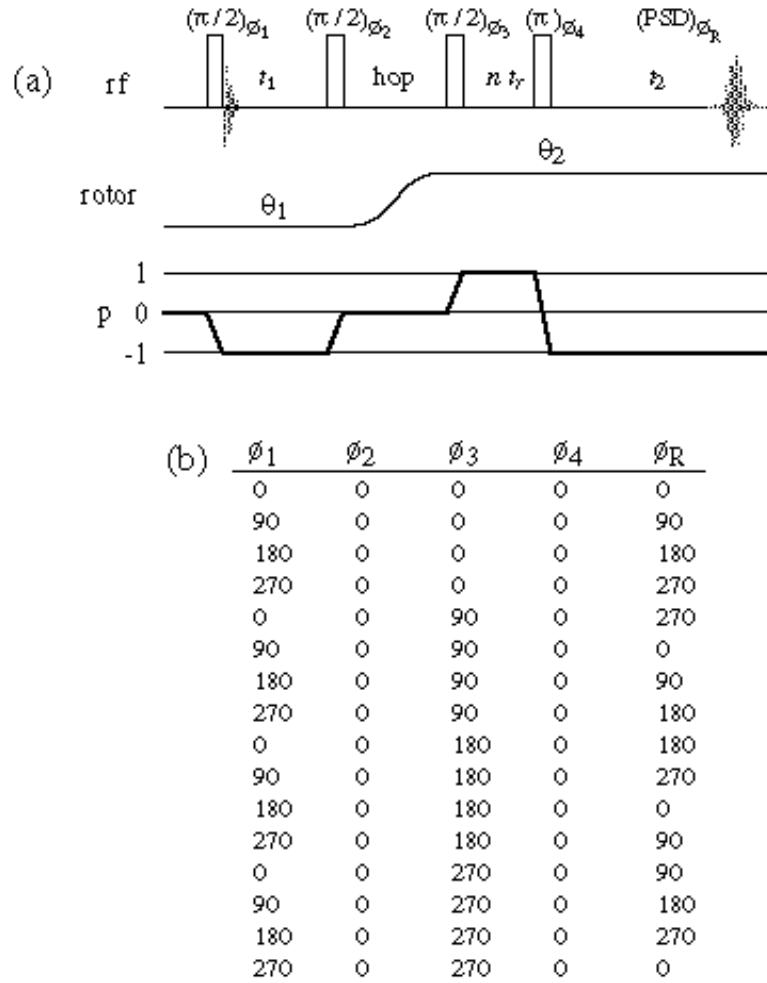
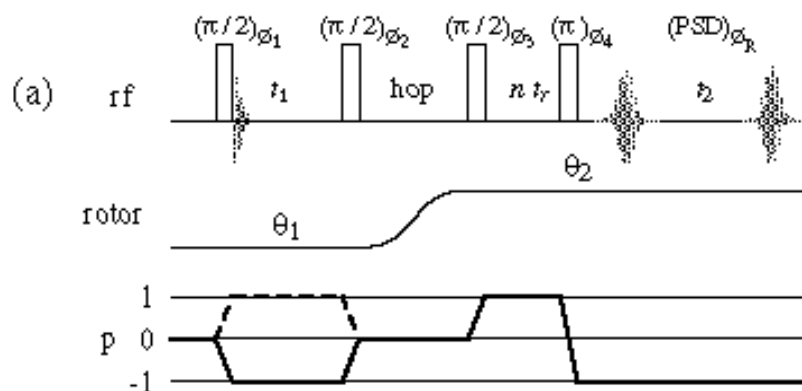


Figure 4.5 Shifted-Echo DAS Experiment. The pulse sequence (a), coherence pathway, and phase cycle (b) are given above.

In cases where the broadening is inhomogeneous in *both* the ω_2 and ω_1 dimensions of a DAS experiment, further advantage may be had by collecting hypercomplex data in concert with a shifted echo experiment. This hypercomplex SEDAS experiment is shown schematically in figure 4.6. The phase cycle for both the cosine and sine portions of the data set are indicated as well. In both the SEDAS and HyperSEDAS experiments, both the first and third pulses are phase cycled through four steps each. This effectively chooses only a -1 (or both +1 and -1 in the hypercomplex division of the phase cycle in figure 4.6) coherence after the first pulse and guarantees a +1 coherence following the third pulse. This sequence effectively collects both the echo and anti-echo DAS

signals. In the case of a crystalline sample, the anti-echo signal will shift to the left in t_2 as t_1 increases while the echo signal will shift to the right in t_2 as t_1 increases.



(b)

ϕ_1	ϕ_2	ϕ_3	ϕ_4	ϕ_R
0	0	0	0	0
180	0	0	0	180
0	0	90	0	270
180	0	90	0	90
0	0	180	0	180
180	0	180	0	0
0	0	270	0	90
180	0	270	0	270

(c)

ϕ_1	ϕ_2	ϕ_3	ϕ_4	ϕ_R
90	0	0	0	0
270	0	0	0	180
90	0	90	0	270
270	0	90	0	90
90	0	180	0	180
270	0	180	0	0
90	0	270	0	90
270	0	270	0	270

Figure 4.6 Hypercomplex Shifted-Echo DAS Experiment. The pulse sequence (a), coherence pathway, and phase cycle for the cosine data set (b) and sine data set (c) are given above. Two echos are shown in the above figure since the signal will have an echo contribution from both the echo (solid line) and anti-echo (dashed line) pathways which may not necessarily occur at the same point.

In this case, the anti-echo will often shift out of the window before decaying to zero intensity in t_1 . In most cases (assuming enough points are taken in t_2) the echo signal will always remain in the observation window. If the $n t_r$ decay is chosen long enough so that

both the echo and anti-echo data remain in the acquisition window for all t_1 points, the total intensity will be nearly zero (in analogy to collecting long delay times in a constant time experiment).

In the case of a sample with a broad inhomogeneous distribution of sites in both dimensions, the echo will decay away much faster in t_1 . In addition, if the distribution in t_1 is continuous, the anti-echo will not shift to the left in t_2 as rapidly in t_1 . Likewise, the echo will not shift to the right in t_2 as quickly in t_1 . For the case of an amorphous solid, the hypercomplex SEDAS is the best pulse sequence, since it combines the signal-to-noise enhancements of an echo in t_2 with hypercomplex data in t_1 . Chapter 8 gives specific examples of glasses with distributions of isotropic shift, for which acquisition with HyperSEDAS gave significant improvements in sensitivity.

Experimental Examples

The following figures (figs. 4.7, 4.8, and 4.9) show examples of various types of DAS spectra. All of these spectra were taken with $k=5$ (the angle pairs were 63.43° and 0.00°) and the magnetic field strength was 11.7T. The sample used was a standard reagent grade RbClO_4 sample. The pulse sequences for each experiment are indicated in each figure caption. The 90° and 180° selective pulses were $3.35 \mu\text{s}$ and $6.70 \mu\text{s}$ respectively, the axis reorientation time was 50 ms, the spinning rate was 5.8 kHz, the echo time in SEDAS and HyperSEDAS experiments was 1.029 ms and the number of acquisitions for each t_1 point was 128 scans for both the sine and cosine data sets. The hypercomplex sine and cosine data sets were combined to produce the normal phase modulated data in t_1 . The dwell time in the t_2 dimension and in the t_1 dimension following proper shearing was $50 \mu\text{s}$ for both. The acquisition length in the second dimension was 256 complex points while it was 128 points in the first dimension.

Figure 4.7 shows the normal phase modulated DAS data set acquired with the pulse sequence in figure 4.2 showing the usual phase-twist lineshape. The phase-twist

lineshape greatly increases the effective linewidth in the anisotropic dimension. In this spectrum (and in figs. 4.8 and 4.9), contours were placed at -12, 14, 41, 68 and 95 percent of the maximum. The negative contours appear to the lower left and upper right of the center of the main peak, just as they occur in figs 4.1b and 4.2.

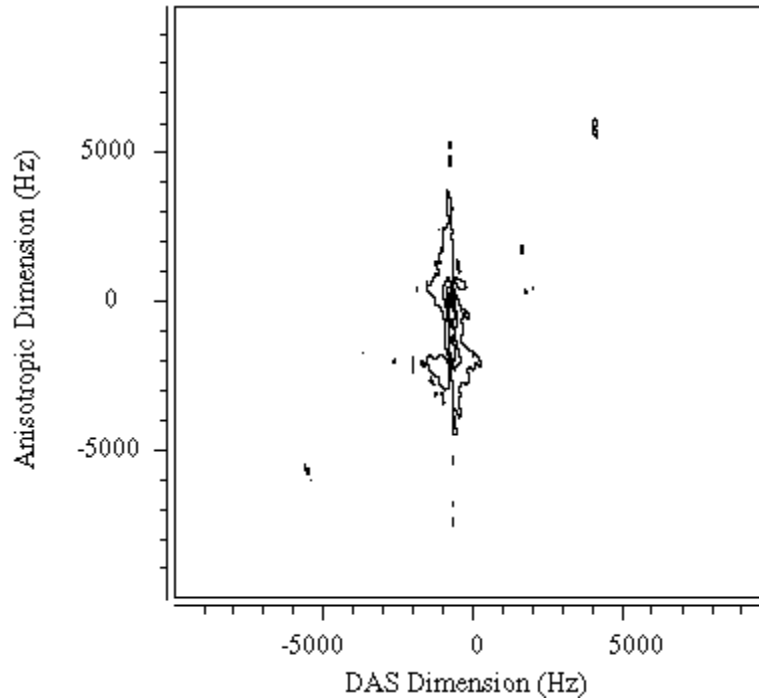


Figure 4.7 Original DAS Spectrum. This spectrum was taken with the parameters given in the text above and with the pulse sequence in figure 4.2.

Figure 4.8 shows the echo DAS spectrum collected with the pulse sequence in figure 4.3. Note that a $41.67 \mu\text{s}$ t_1 dependent first-order phase correction was required to shear the two-dimensional spectrum. This spectrum is not quite completely pure-absorptive phase. However, the dispersive contributions are of small enough size that they do not change the overall appearance of this spectrum in reference to the completely pure-absorptive phase spectrum in figure 4.9.

Figure 4.9 shows the pure-absorptive spectrum acquired with the hypercomplex DAS pulse sequence (figure 4.4). The spectra acquired with SEDAS and HyperSEDAS look virtually identical and are not shown. The lineshape shows no phase-twist dispersive components in the two-dimensional spectrum above.

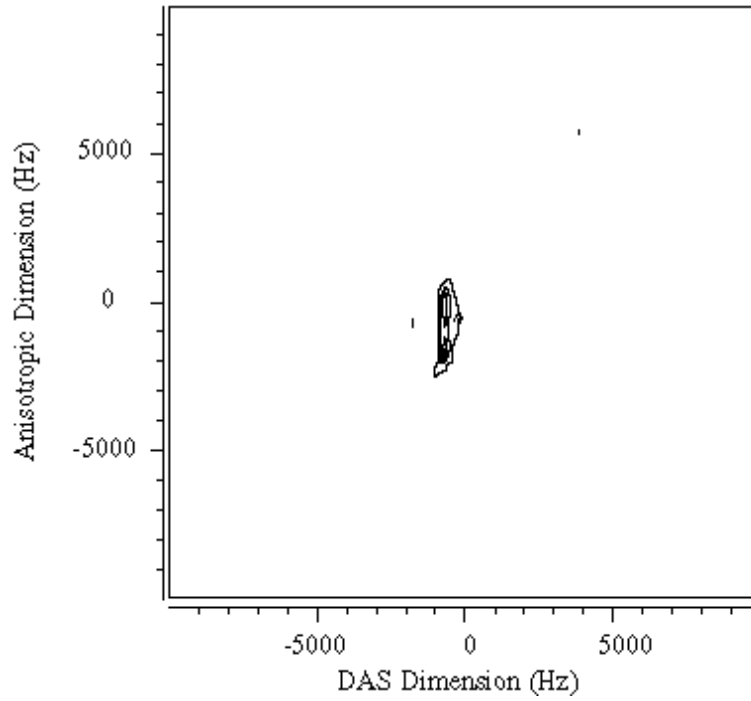


Figure 4.8 Echo DAS Spectrum. This spectrum was taken with the pulse sequence given in figure 4.3.

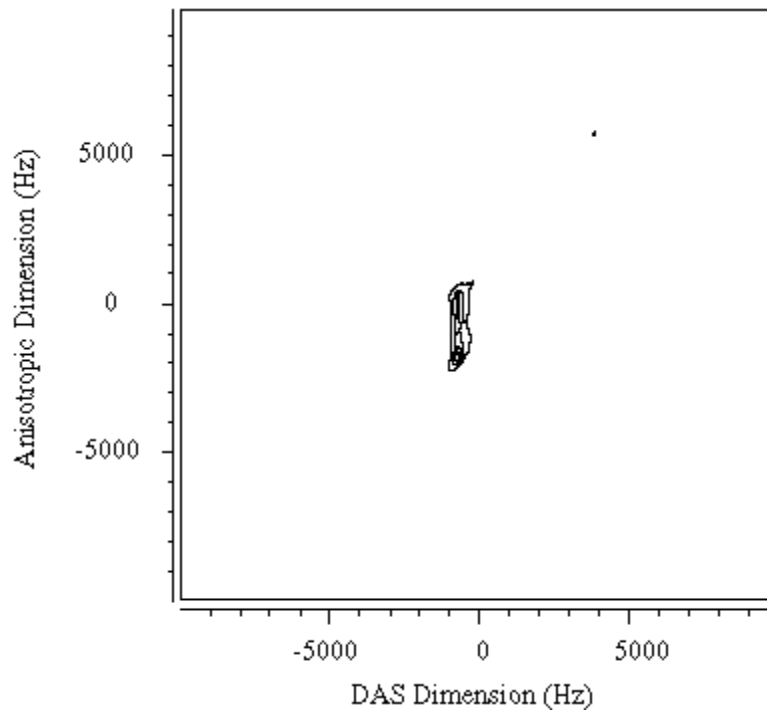


Figure 4.9 Hypercomplex DAS Spectrum. This spectrum was taken with the pulse sequence given in figure 4.3.

Signal-to-Noise Ratio Enhancements

In the case of one-dimensional DAS spectra, the signal-to-noise enhancement will be independent of the enhancement in the anisotropic dimension. In practice, the shifted echo experiments will provide better signal-to-noise, since the complete DAS echo signal can be collected for short t_1 points. For short t_1 points in the non-shifted DAS experiments, the echo top intensity may be complicated by ringing of the probe. This ringing can significantly reduce the signal-to-noise ratio in the one-dimensional projections. Also, by doing only a partial projection of the signal in the two dimensional spectrum (rather than a complete projection) by adding only regions with strong signal, significant improvements in signal-to-noise ratio in the one dimensional DAS spectra may be achieved. This may distort the overall intensities in the final DAS spectrum and in some cases it is not possible to eliminate any region of the two dimensional spectrum for projection.

In table 4.1, the two dimensional signal-to-noise ratios are tabulated for each of the various DAS pulse sequences. These numbers are arrived at by measuring the RMS noise in a region of the 2D spectrum which is devoid of signal and comparing this to the highest point (largest signal) in the complete 2D spectrum. The experimental examples shown in the previous section were used to generate these ratios. As has been predicted by theory, the hypercomplex SEDAS experiment has the highest signal-to-noise ratio. This should in theory be a factor of $\sqrt{2}$ 1.4 better than the SEDAS experiment. In this case, the factor was indeed achieved, but in practice this may not be always be true, since the DAS anti-echo may shift out of the acquisition window too rapidly. The SEDAS signal-to-noise ratio should also be a factor of $\sqrt{2}$ 1.4 better than both the echo DAS and hypercomplex DAS experiments.

Sequence	Pure Phase	S/N Ratio
z-Filter DAS	yes	15.8
DAS (fig. 4.2)	no	20.6
Hypercomplex DAS (fig. 4.4)	yes	31.3
Echo DAS (fig. 4.3)	no	31.6
Anti-echo DAS (fig 4.3, dashed pathway)	no	10.9
Shifted-echo DAS (fig. 4.5)	yes	43.4
Hypercomplex Shifted Echo (fig. 4.6)	yes	67.0

Table 4.1 Signal-to-Noise Ratio Enhancements For a Variety of Pulse Sequences. These measurements were all performed with equal acquisition time for each experiment.

Again, this enhancement seems to hold quite well. The hypercomplex DAS should be better by a factor of $\sqrt{2}$ 1.4 than the original DAS experiment, which also is true. Finally the z-filter pure phase method signal-to-noise ratio should be comparable to the original DAS experiment, since the z-filter sacrifices a factor of $\sqrt{2}$ 1.4 which is restored by the hypercomplex data collection. In practice, the z-filter will have worse signal-to-noise ratios than the original phase modulated data, since relaxation during the z-filter will further reduce the signal-to-noise in this type of experiment. Therefore, theory predicts that the signal to noise of the hypercomplex SEDAS will be at least a factor of $\sqrt{8}$ 2.8 better than the older z-filter method of acquiring pure-phase data. A final comment about pure-absorption phase DAS is to warn the reader that in some cases SEDAS or hypercomplex DAS may actually work better than the full hypercomplex SEDAS. This will occur when the apparent T_2 of a sample is too fast to allow long $n t_T$ echo times. In most cases throughout this thesis, the SEDAS pulse sequence will be used.